Refractory Element Fractionations in the CV3 Carbonaceous Chondrite Allende: What Role do CAIs Play?

Marc Lipella
Dr. Roberta Rudnick
Dr. William McDonough
Dr. Richard Ash
Dr. Philip Piccoli

Abstract

Several studies, primarily Kornacki and Fegley (1986) and Munker et. al. (2003), suggested that calcium-aluminum-rich inclusions (CAIs) common to the CV3 subclass of chondritic meteorites contain significantly lower Nb-Ta ratios than the accepted bulk solar system value. These studies have lead me postulate that; *CV3 carbonaceous chondrites display, on average, low Nb/Ta values because of the low Nb/Ta values in the CAIs.* Calcium, titanium, niobium, tantalum, zirconium, and hafnium abundances were obtained via LA-ICP-MS analysis on five chondrules, two CAIs, and the matrix from the CV3 carbonaceous chondrite Allende. The matrix displayed Nb/Ta and Zr/Hf values that encompass around the accepted bulk solar system values of 19.9 $\pm$ 2 and 34.3 $\pm$ 3.5 respectively. The chondrules extracted from Allende displayed variable Nb/Ta values that ranged from 3.8 to 24.2 ($1\sigma = 10\%$), and Zr/Hf values that ranged from 30.4 to 41.0 ($1\sigma = 10\%$). The CAIs displayed consistently low Nb/Ta values that ranged from 0.9 to 12.7 ($1\sigma = 10\%$), and erratic Zr/Hf values that ranged from 12 to 73 ($1\sigma = 10\%$). The Nb-Ta ratios in comparison with the Zr-Hf ratios show evidence that fractionation of Nb and Ta occurred independently of any Zr and Hf fractionation. Furthermore, within CAIs, there is evidence that as the Nb/Ta values decrease, the Zr/Hf values become more erratic. I cannot say that I know the reasons behind these low Nb/Ta values, nor the erratic Zr/Hf values found within these CAIs, I speculate that any inaccuracy in the currently accepted 50% condensation temperatures of these refractory elements may provide insight into the mechanisms behind the findings in this study.

1. Introduction

On the 8th of February 1969 the Allende meteorite collided with the Earth in northern Mexico. Since the fall of Allende, it has become one of the most researched and publicized meteorites in cosmochemical science; not just because there is a vast abundance of material, but it turns out that Allende happens to belong to a class of chondrite that contains an abundance of calcium-aluminum-rich inclusions (CAIs). CAIs exhibit unique textural, mineralogical, and compositional characteristics, primarily and abundance of refractory elements. CAIs are of one of the first known materials to condense out of the high temperature solar nebula (Grossman, 1973). The radiogenic isotope ^{26}Al has a half-life of 730,000 years and decays to ^{26}Mg. ^{26}Mg excesses in CAIs indicate that the ^{26}Al isotope, present when the CAIs formed, had all but decayed by the time most other materials formed (Ash, McDonough, and Rumble III 2003). This indicates that the CAIs formed prior to their inclusion in chondrites.

Whereas CAIs are demonstrated to be one of the oldest materials in the solar system, it is uncertain how they formed or how they are related to other material. In fact, the formation of CAIs is currently a widely debated topic in cosmochemistry. Many researchers have obtained excellent data on rare-earth-element (REE) abundances and their patterns in CAIs, whereas analyses of non-REE refractory elements have been scarce, especially data for Nb and Ta, two elements considered to display minimal amounts of fractionation. However, Kornacki and Fegley (1986) and Munker et. al. (2003) obtained Nb and Ta data that display evidence of fractionation, indicated by a Nb/Ta value significantly lower than that of the accepted bulk solar system value.

Obtaining accurate and precise data on the refractory elements Nb, Ta, Zr, and Hf on several different CAIs may assist in the understanding of why these fractionations occur, and may shed some light on the conditions and mechanisms behind CAI formation and how they relate to chondrules and other chondritic constituents. Additionally, looking at refractory element abundances in relatively unaltered material can provide information on their whereabouts in the primitive Earth (i.e. before differentiation), as well as the present Earth.

2. Background

Refractory elements are elements with high condensation temperatures, with values greater than that of metallic iron (Wanke et. al., 1974). The accepted 50% condensation temperature for metallic iron is approximately 1350K. Volatile elements, the antithesis of refractory elements, have considerably lower condensation temperatures. Refractory elements can be further classified as siderophile, lithophile, or chalcophile elements. Siderophile elements prefer to reside in metal phases and are primarily found in the cores of differentiated bodies. Lithophile elements frequently bond with oxygen and reside predominantly in the silicate portion of a differentiated body. Chalcophile elements favor bonds with sulfur. These distributions are the same in undifferentiated bodies, like Allende, as well.

A meteorite is some portion of an extraterrestrial rock body that survives the passage through the Earth’s atmosphere. Before contact with Earth, a meteorite is known as a meteoroid. Meteoroids can be portions of matter created during solar system formation that never accreted into a planet, or a portion of another body in space that has been broken apart. Meteorites actually played a significant role in planetary formation during the earlier stages of our solar system. During the first half billion years of Earth’s history it experienced a period of intense meteoritic bombardment. In fact some argue that planets are formed completely out of aggregated meteoritic bodies.

Chondrites are meteoritic bodies that exhibit no evidence of any planetary differentiation, and are characterized by a mixture of matrix, chondrules, and, commonly in carbonaceous chondrites Calcium-Aluminum-rich Inclusions (CAIs). Carbonaceous chondrites are chondrites that generally formed in more oxidizing environments, and have the largest proportion of volatile elements. The CV3 subclass of carbonaceous chondrites is characterized by large chondrules and CAIs. Chondrules are small millimeter-sized igneous spheres that have both melted and crystallized within the realm of space. CV chondrites also have a high abundance (~ 10%) of CAIs, first described in a CV meteorite that fell in Vigarano, Italy. CAIs are clasts within chondrites that contain different chemical and mineralogical characteristics than all other chondritic components, primarily a relatively high abundance of refractory elements. CAIs can be further broken down in to type A and type B CAIs. Type A CAIs contain higher refractory element concentrations. Type B CAIs are more Al-Ti-rich. The meteoritic matrix can be looked at as the cement that holds both the chondrules and the CAIs together within the chondrite. The matrix is primarily a constituent of very fine-grained material containing fragments of CAIs and chondrules, as well as sulfides, metals, organic material, alteration products, and presolar grains.

3. What Niobium, Tantalum, Zirconium, and Hafnium Have to Tell Us

Nb, Ta, Zr, and Hf are all refractory elements -- elements originally thought to reveal a minimal amount of relative fractionation during cosmochemical and geochemical processing. The 50% condensation temperatures for Nb and Ta are 1557K and 1565K respectively. Zr and Hf have slightly higher 50% condensation temperatures at 1741K and 1676K respectively (Lodders 2003). Niobium and tantalum easily substitute for one another, have 5+ valence states, have the same ionic radii, and have electronegativities that differ by only one-tenth. These parameters are important because they govern ionic substitution laws. Zr and Hf share a similar ability to substitute for one another as Nb and Ta do, with the only exception that their electronegativites vary by slightly more, 0.6. Goldschmidt's rules of substitution state that in order for elements to substitute for one another freely their valence numbers can differ by only one, and their atomic radii need to vary by <15%. Given these parameters, wherever Nb can be found, Ta should be there as well, and any crystallographic position that Zr holds, Hf can possess.

Niobium has only one naturally occurring isotope, ^{93}Nb. Tantalum only has two ^{181}Ta and ^{180}Ta, with ^{181}Ta occurring as 99.998% of all naturally occurring Ta (Thomas *PartXII* 25). Lastly, they have no isobaric overlaps at their respective mass numbers of 93 and 181. This helps decrease the possibility of analytical interferences common when using a mass spectrometer, and helps increase the accuracy of the data received from the instrument.

4. Previous Research

Several studies have sparked scientific interest in the study of refractory element fractionations in chondrites and early nebular condensates. Kornacki and Fegley (1986) studied the abundances of siderophile and lithophile refractory trace elements in CAIs, and recorded a range of Nb/Ta values that varied from 17.92 to 3.61. This spread of values is substantial enough to suggest fractionations of niobium and tantalum. However, these data are open for interpretation. The data were obtained compiled from several studies, which may or may not have used similar instrumentation, had similar standards of study, and/or studied the same CAIs. Potential inconsistencies in data collection could result in an error of great enough magnitude to challenge the findings of this study. Table 1.1 displays the mean abundance data for CAIs from individual studies compiled by Kornacki and Fegley, and their method of analysis. As can be seen only Wanke (1947) and Grossman (1976) used the same method of analysis, gamma-ray spectrometry. Additionally, Wanke et. al. (1974) was the only study to analyze both Nb and Ta measured on the same CAI, reporting Nb-Ta ratios similar to that of the bulk solar system values, indicating no evidence for fractionation, however the errors were large.

More recently, Munker et. al. (2003), ascertained bulk Nb/Ta values for various classes of chondrites in order to determine the bulk solar system Nb/Ta value. They established a mean overall average for the solar system that was higher than previously established in a study performed by Jochum et. al. (1986). In contrast, Munker et. al. (2003) found that CV3 carbonaceous chondrites displayed significantly lower Nb/Ta ratios than that found in all others, with ratios around 17 versus ratios around 20 for all other classes. They suggested that this was due to the high abundance of CAIs, common to that subclass of chondrite, which contributed to the low Nb-Ta ratios, and that overall CAIs have low Nb/Ta values (Munker et. al. 2003). Given the information acquired from these two studies I deduced my hypothesis. *CV3 carbonaceous chondrites display, on average, low Nb/Ta values because of the low Nb/Ta values in the CAIs.*

Element Abundance Data Collected in the Various Studies that Kornacki and Fegley (1986) Cited in Their Research

Study	Nb	Ta	Nb/Ta	Zr	Hf	Zr/ Hf	Method of Analysis
Mason (1982)	3.9 ±5%	n.d.	n.d.	61 ±5%	1.9 ±5%	32 ±7%	Spark-Source Mass Spectromotry
Grossman (1977)	n.d.	n.d.	n.d.	50 ±10%	n.d.	n.d.	Collected from a previous study
Wanke (1974)	6.6 ±20%	0.25 ±20%	26 ±28%	93 ±10%	3.3 ±10%	28 ±14%	Gamma-ray spectrometry
Grossman (1976)	n.d.	0.29 ±42%	n.d.	n.d.	1.7 ±24%	n.d.	Gamma-ray spectrometry

Table 1.1: Refractory element abundance data measured on CAIs from the various sources Kornaki and Fegley (1986) used to compile their values. Included are the abundance data (ppm), the study conducted, and the means of analysis. The values on this table represent the mean values as reported in these studies. The errors represent the largest error reported for any of the data obtained for that individual element.

5. Procedure

The first step in the procedure was to obtain samples of CAIs from the CV3 chondrite, Allende. I received four samples containing seven CAIs, courtesy of the National Museum of Natural History in Washington, D.C. These samples were sent out to be made into thick, polished-sections of 50 microns in thickness. Thick-sections are more advantageous than grain-mounts or thin-sections in this study for several reasons. Both microprobe and laser ablation inductively coupled plasma mass spectroscopy (LA-ICP-MS) analyses can be undertaken directly from the slide, unlike thin-sections where there is a fair chance that the laser may ablate entirely through the sample before obtaining sufficient counts to assure accuracy and precision. Additionally, thick-sections can be analyzed with a petrographic microscope, an option not possible with grain-mounts.

The optical petrography proved to be quite difficult via microscope due to the very fine-grained texture of many CAIs. Reflected light imaging and backscattered electron (BSE) images proved to be the most useful in defining the grain boundaries of the various phases. Reflected light optics are obtained from a petrographic microscope that directs light to the top of a slide; the light is then reflected back into the microscope's objective. Backscattered electron images reflect the mean atomic number of a present phase. The image is observed in grayscale, where the darker shades have lower mean atomic numbers, and the lighter areas reflect higher mean atomic numbers. Two CAIs were chosen for in-depth analysis because they initially appeared to be course-grained enough so that individual phases could be analyzed via laser (minimum spot size of 30 microns) to determine that if any fractionation of Nb and Ta occurs, and whether it is confined to a specific phase or the bulk CAI. The primary phases present in these CAIs, determined by a combination of semi-quantitative microprobe analysis and optical petrography, are spinel, anorthite, melilite, and a calcium-rich pyroxene (see Table 2.1 for stoichiometry).

Stoiciometry of the Primary Phases Found in the CAIs]

Phase	**Stiochiometry**
Melilite	$Ca_2Al(Al,Si)O_7$ $Ca_2MgSi_2O_7$
Anorthite	$CaAl_2Si_2O_8$
Calcium-rich pyroxene (fassite)	$Ca(Mg,Al,Ti)(Al,Si)_2O_6$
Spinel	$MgAl_2O_4$

Table 2.1: The primary phases found within the CAIs analyzed via optical petrography and qualitative microprobe analysis and their relative stoichiometries.

After microprobe analysis of the two selected CAIs I discovered that many of the grains are entirely too small (<30 microns) to analyze reliably via LA-ICP-MS. This problem was solved by assuming a standard laser spot size of 30 microns, then going back to the microprobe and using a 30 micron beam to obtain bulk qualitative data at various points within the CAIs. Although this method did not allow me to determine whether or not Nb-Ta fractionation is phase-specific, major element abundances for the area are determined and can be used to normalize the data acquired from the LA-ICP-MS. Normalization of the LA-ICP-MS data allows for the determination of the exact abundances of the elements analyzed by the instrument. Titanium was chosen as the internal standard due to its relatively consistent abundance (~1 wt%) and its ease and ease of analysis by LA-ICP-MS.

Refractory element concentrations were determined by LA-ICP-MS analysis at the University of Maryland. This instrumentation analyzes substances by ablating the solid sample into fine particles suspended in a He gas stream. The particle-charged gas stream is transported by a narrow tube and into the argon plasma of the mass spectrometer. The ablated material is disassociated and ionized by the argon plasma; ions are focused and accelerated down the mass spectrometer flight tube, through a magnetic field that separates ions by mass, and then through an electrostatic analyzer that acts as an energy filter. The ions then hit a conversion dynode, producing electrons that are amplified by an electron multiplier and counted.

In order to discern any Nb-Ta or Zr-Hf ratio fractionations, the three major chondritic constituents were separately analyzed: CAIs, chondrules, and matrix. Multiple samples of all of these constituents were analyzed several times in order to assure both accuracy and precision, as well as providing evidence for, and against, homogeneity within each constituent. The raw data were normalized to the known titanium concentrations determined by microprobe analysis. The normalization converts the raw count data from the mass spectrometer into the actual abundances. With these abundances the Nb-Ta and Zr-Hf ratios can then be calculated. These Nb/Ta and Zr/Hf ratios were compared against various chondritic constituents (i.e. CAI vs. chondrule, or CAI vs. matrix), and to each other (i.e. CAI vs. CAI, or chondrule vs. chondrule). The experimental uncertainty was determined to be ±7% at 1σ for the individual elemental abundances by Poisson's counting statistics, and ±10% at 1σ for their respective ratios by sum of the errors in ratios. Poisson's counting statistics relates the number of counts the ICP-MS obtains on a specific mass number to the uncertainty of the data received. This method of determining uncertainty was used in this study because it produces the largest uncertainty value for the instrumentation I used to obtain the data.

6. Results

Refractory element abundance data for chondrules, CAIs, and matrix from the Allende meteorite are given in Tables 3.1, 4.1, 4.2, and 5.1, and were compiled collectively into one table (Table 6.1) that can be found in the appendix. Backscattered electron images of the five chondrules studied can be seen (Figure 1.1) below. The very bright spots are most likely to be metals and sulfides. The gray shades most likely represent feldspars, pyroxenes, and olivine. The dark areas represent the mesostasis (glass) and holes.

<u>Allende Chondrules A3-A7</u>

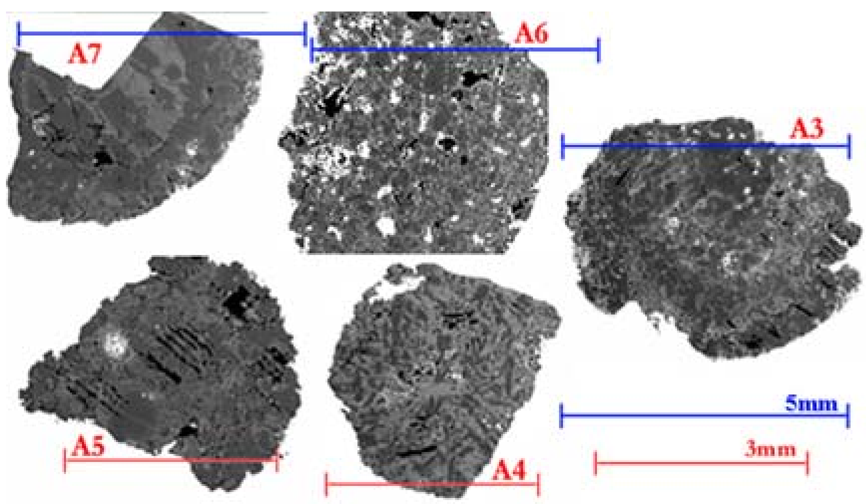

Figure 1.1: Backscattered electron (BSE) images of the five chondrules analyzed via electron microprobe.

Concentrations of Ca, Ti, Zr, Nb, Hf, and Ta were obtained for these five chondrules using the LA-ICP-MS, with Ca and Ti used as internal standards. Spot sizes ranging from 40 μm to 120 μm were selected. Differing spot sizes do not affect the analyses. A larger spot size will increase the number of counts recorded by the instrument, but when the standard values are accounted for in data compilation, the elemental abundance data extrapolates down to the same values. This makes choice of spot size merely a matter of assuring that a sufficient number of counts are achieved for an element given the phase of analysis.

The Nb-Ta ratios I obtained (Table 3.1) vary significantly, ranging from 24.2 to 3.8 (nearly a factor of three variation), whereas, the Zr-Hf ratios varied less, ranging from 34.8 to 41.0 (~15% variation). The experimental uncertainty for both ratios was approximately ±10%, determined using Poisson's counting statistics and the sum of the errors in ratios. The range in Zr/Hf is barely beyond analytical uncertainty.

Refractory Element Ratios in Allende Chondrules

Chondrule	Phases	Spot Size	Nb/Ta ($1\sigma = 10\%$)	Zr/Hf ($1\sigma = 10\%$)
A7	Rim	40 μm	22.3	38.1
	Mes	120 μm	24.2	41.0
A6	Ol + Mes	80 μm	17.7	39.2
	Ol + Mes	120 μm	16.3	39.2
A5	Ol + Px	80 μm	10.4	30.4
A4	Ol + Plag + Px	80 μm	3.8	39.4
A3	Ol + Px	120 μm	10.0	37.6
	Ol + Px	120 μm	7.5	34.8

Table 3.1: Refractory element ratios for single analysis points as determined by LA-ICP-MS for the five Allende chondrules analyzed. Mes = Mesostasis, Ol = Olivine, Px = Pyroxene, and Plag = Plagioclase.

Elemental abundance data for Ca, Ti, Nb, Ta, Zr, and Hf were obtained via LA-ICP-MS analyses on the two selected CAIs as well as several regions within the meteorite matrix (Tables 4.1, 4.2, and 5.1). Laser spot sizes ranging from 30μm to 40μm were used to ablate the samples. Ca and Ti abundance data were obtained in order to normalize the data. The matrix has Nb/Ta values mostly within the error of chondrite (Table 5.1), with values of 16.2 and 20.5 (chondritic = 19.9 ± 2). The Zr/Hf values obtained were 34.7 and 41.0, with the latter being just above the error of chondrite (chondritic = 34.3 ± 3.5).

Refractory Element Ratios in Allende Matrix

Point Name	Nb/Ta (1σ = 10%)	Zr/Hf (1σ = 10%)
Matrix1	16.2	34.7
Matrix2	20.5	41.0

Table 5.1: Refractory element ratios for single analysis points as determined by LA-ICP-MS analysis for the matrix of the CV3 chondrite Allende.

The CAIs on the other hand displayed significantly lower (up to an order of magnitude) Nb/Ta values than that of chondritic, with the 1σ error of 10% taken into consideration (Tables 4.1 and 4.2). The CAI in sample 3529-63-RR1 has Nb-Ta ratios that range from 2.9 to 12.2, with an average of 5.0, and the Zr-Hf ratios that range from 29 to 64, with an average of 47 (Table 4.1). The sample in CAI 3529-61-RR1 has Nb-Ta ratios that range from 0.9 to 12.7 with an average of 4.7, and the Zr-Hf ratios range from 12 to73 with an average of 47 (Table 4.2). Overall, the Nb-Ta ratios range from 0.9 to 12.7 with a mean value of 4.7, and the Zr-Hf range from 12 to 73 with a mean value of 47.

CAI Refractory Element Concentrations and Ratios in Sample 3529-63-RR1

Point Name	Nb (ppm) (1σ = 7%)	Ta (ppm) (1σ = 7%)	Nb/Ta (1σ = 10%)	Zr (ppm) (1σ = 7%)	Hf (ppm) (1σ = 7%)	Zr/Hf (1σ = 10%)
B03	3.42	0.98	3.5	20.6	0.44	46.7
B04	1.25	0.36	3.5	8.72	0.17	52.7
B05	1.87	0.33	5.7	2.29	n.d.	n.d.
B06	2.92	1.06	2.7	24.1	0.38	63.8
B07	1.05	0.32	3.3	8.55	0.17	49.7
B08	7.34	1.04	7.1	35.3	0.62	56.8
B09	3.45	0.70	4.9	25.1	0.64	39.1
B10	1.08	0.27	4.0	9.28	0.23	41.1
B11	1.91	0.56	3.4	11.5	0.25	46.2
B12	1.22	0.27	4.6	1.24	n.d.	n.d.
B13	1.60	0.23	7.0	13.8	0.48	28.7
B14	2.36	0.19	12.2	14.5	0.32	44.9
B15	0.57	n.d.	n.d.	n.d.	0.07	n.d.
B16	0.90	0.31	2.9	n.d.	n.d.	n.d.
Chondritic	-	-	19.9	-	-	34.3

Table 4.1: Refractory element concentrations in ppm and their respective ratios for single analysis points of the CAI in the sample 3529-63-RR1. The point name merely serves as a reference for the area analyzed via LA-ICP-MS and can be correlated to Figure 3.1 in the appendix.

CAI Refractory Element Concentrations and Ratios in Sample 3529-61-RR1

Point Name	Nb (ppm) (1σ = 7%)	Ta (ppm) (1σ = 7%)	Nb/Ta (1σ = 10%)	Zr (ppm) (1σ = 7%)	Hf (ppm) (1σ = 7%)	Zr/Hf (1σ = 10%)
A05	3.62	1.81	2.0	19.5	n.d.	n.d.
A06	0.14	0.06	2.4	0.62	0.05	11.8
A07	0.70	0.44	1.6	4.27	0.07	61.4
A10	0.35	0.40	0.9	1.31	0.03	43.9
A11	0.31	0.13	2.5	1.68	0.03	48.8
A12	1.69	1.08	1.6	6.37	0.09	73.1
A13	2.78	0.87	3.2	10.7	0.16	65.3
A16	0.65	0.05	12.7	5.70	0.18	31.2
A17	0.03	0.003	10.2	0.16	0.004	37.2
A18	0.57	0.11	5.2	18.4	0.44	41.4
A19	0.45	0.05	9.8	3.39	0.07	51.0
Chondritic	-	-	19.9	-	-	34.3

Table 4.2: Refractory element concentrations in ppm and their respective ratios for single analysis points of the CAI in the sample 3529-61-RR1. The point name merely serves as a reference for the area analyzed via LA-ICP-MS and can be correlated to Figure 3.2 in the appendix.

7. Interpretations

When the data obtained on the various chondritic constituents is compared, the results become quite interesting. The refractory element data for the chondrules display Nb-Ta ratios that vary significantly from chondrule to chondrule. The three chondrules that were analyzed in multiple areas display relatively consistent Nb/Ta values internally. The chondrule labeled A4 displays a significantly low Nb-Ta ratio. This chondrule is enriched in aluminum and calcium, presumably due to the presence of both plagioclase and spinel, two phases that contain abundant Al and Ca. Ash et. al. (2003) measured rare-earth element (REE) abundances twenty chondrules from Allende, including the five I analyzed here. They found that the REE for most chondrules were in chondritic relative abundances, ranging from half to twice that of the bulk solar system composition. However, the A4 chondrule displays an erratic REE pattern with anomalies in Eu, Ho, and Er that are fractionated by more than an order of magnitude from the bulk solar system values. These REE patters are said to be definitive of that found in Group II CAIs (Ash et. al., 2003).

Refractory element data obtained for the CAIs in Allende display consistently low Nb/Ta values both internally and in comparison with each other. The Zr-Hf ratios in the CAIs are erratic, varying from below chondritic to significantly above it. Unlike the chondrules and the CAIs, the matrix diplays near chondritic values for both Nb/Ta and Zr/Hf. Additionally, any Nb/Ta fractionations observed appear to be completely independent of any Zr/Hf fractionations. Figure 2.1 is a graph displaying the Nb/Ta values versus the Zr/Hf values. If the two ratios were to have similar fractionation patterns the data points would all be in the same relative area, and this is not the case. The CAI Zr/Hf values also appear to be more erratic in areas that have low Nb/Ta values.

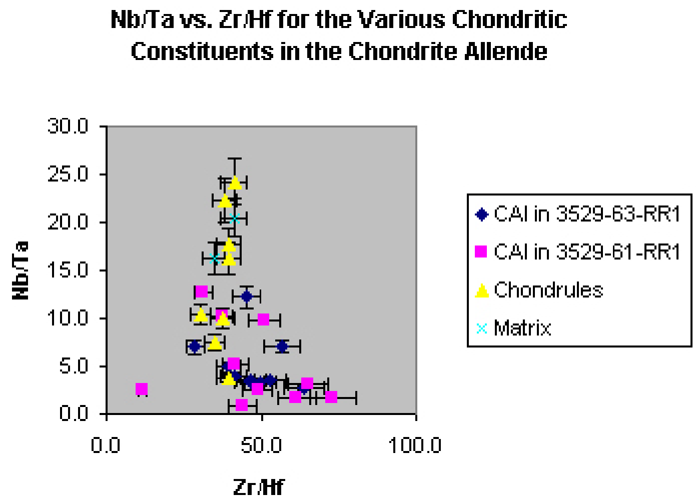

Figure 2.1: Nb/Ta values versus Zr/Hf ratios obtained via LA-ICP-MS for the various chondritic constituents studied.

The data provide strong evidence to support my hypothesis that *CV3 carbonaceous chondrites display, on average, low Nb/Ta values because of the low Nb/Ta values in the CAIs.* I cannot say that I know the reasons behind these low Nb/Ta values, nor the erratic Zr/Hf values found within these CAIs. One possibility is that the 50% condensation temperatures, as discussed in section 3, are inaccurate. The 50% condensation temperatures of nearly all elements are calculated theoretically using solar elemental abundances and various thermodynamic properties (Lodders 2003). Our understanding of the extreme conditions that these refractory elements experience in the high temperature solar nebula may be inaccurate, leading to an inaccuracy in the calculated 50% condensation temperatures. There are still many frontiers of research on CAIs and their formation that need to be explored before we can comfortably and confidently say that we have a good understanding as to their formation, and the resultant significance of it.

Acknowledgements

I would like to thank Dr. Roberta Rudnick, Dr. William McDonough, Dr. Richard Ash, and Dr. Philip Piccoli at the University of Maryland for their continual guidance and good company throughout the progress of this study, I could not have done it without them. Dr. Glenn MacPherson for his generous assistance and the Allende samples analyzed. Dr. Tim McCoy, Linda Walzenbach, and the National Museum of Natural history for the samples of Allende. I would additionally like to thank Tim Rose for cutting the samples and Don Resultay for making the thick-sections.

References

Ash R.D., McDonough W.F., and Rumble III D. "Rare Earth Elements and Oxygen Isotopes in Allende Chondrules as evidence for CAI mixing in Chondrule Precursors." Lunar and Planetary Science. 34: (2003).

Brearley and Jones. "Chondritic Meteorites." Planetary Materials. Ch. 3: 83-107.

Brenan J.M., McDonough W.F., and Dalpe C. "Experimental Constraints on the Partitioning of Rhenium and Some Platinum-Group Elements Between Olivine and Silicate Melt." Earth and Planetary Science Letters. 212 (2003): 135-150.

Chou C., Baedecker P.A, and Wasson J.T. "Allende Inclusions: Volatile-Element Distribution and Evidence for Incomplete Volatilization of Presolar Solids." Geochimica et Cosmochimica Acta. 40 (1976):85-94.

Connolly Jr., Harold C. and Love, Stanley G. "The Formation of Chondrules: Petrologic Tests of the Shockwave Model." Science. Vol. 280. 3 Apr 1998: 62-67.

Grossman, L. "Refractory Trace Elements in Ca-Al-Rich Inclusions in the Allende Meteorite." Geochimica et Cosmochimica Acta. 37 (1973): 1119-1140.

Grossman L. and Ganapathy R. "Trace Elements in the Allende Meteorite – I. Coarse-Grained, Ca-rich Inclusions." Geochimica et Cosmochimica Acta. 40 (1976a): 331-334.

Grossman L. and Ganapathy R. "Trace Elements in the Allende Meteorite – II. Fine-Grained, Ca-rich Inclusions." Geochimica et Cosmochimica Acta. 40 (1976b): 967-977.

Grossman L., Ganapathy R., and Davis A.M. "Trace Elements in the Allende Meteorite – III. Coarse-Grained Inclusions Revisited." Geochimica et Cosmochimica Acta. 41 (1977): 1647-1664.

Jochum et. al. "The Solar-System Abundances of Nb, Ta, and Y, and the Relative Abundances of Refractory Lithophile Elements in Differentiated Planetary Bodies." Geochimica et Cosmochimica. Vol. 50. 6 Mar. 1986: 1173-1183.

Kornacki, A. S. and Fegley Jr., B. "The Abundance and Relative Volatility of Refractory Trace Elements in Allende Ca,Al-Rich Inclusions: Implications for Chemical and Physical Processes in the Solar Nebula." Earth and Planetary Science Letters. 79 (1986): 217-234.

Krot et. al. “A New Astrophysical Setting for Chondrule Formation.” Science. Vol. 291. 2 Mar 2001: 1776-1779.

Lodders, K. “Solar System Abundances and Condensation Temperatures of the Elements.” The Astrophysical Journal. 591 (2003): 1220-1247.

Longerich et. al. “Laser Ablation Inductively Coupled Plasma Mass Spectrometric Transient Signal Data Acquisition and Analyte Concentration Calculation.” Journal of Analytical Atomic Spectrometry. Vol. 11. Sep 1996: 899-904.

Lord H.C. III. “Molecular Equilibria and Condensation in a Solar Nebula and Cool Stellar Atmospheres.” Icarus. 4 (1965): 279-288.

MacPherson, G. J. “Calcium-Aluminum-Rich Inclusions in Chondritic Meteorites.” Treatise on Geochemistry. Volume I. (2003): 201-246.

Mason B. and Taylor S.R. “Inclusions in the Allende Meteorite.” Smithsonian Contributions to the Earth Sciences. 25 (1982): 1-30.

McDonough, W.F. et. al. “Lithium Isotopic Composition of Chondritic Meteorites.” Lunar and Planetary Science. 24: (2003).

McSween Jr., H. Y. “Meteorites.” The New Solar System. Fourth Edition. Ed. Beatty, Collins-Petersen, and Chaikin. Cambridge: Sky Publishing, 1999. 351-363.

Munker et. al. “Evolution of Planetary Cores and the Earth-Moon System from Nb/Ta Systematics.” Science. Vol. 301. 4 Jul. 2003: 84-87.

Nagasawa et. al. “Trace Element Distribution in Mineral Separates of the Allende Inclusions and Their Genetic Implications.” Geochimica et Cosmochimica Acta. 41 (1977): 1587-1600.

Nagasawa et. al. “Trace Element Concentrations in the Isotopically Unique Allende Inclusion, EK 1-4-1.” Geochimica et Cosmochimica Acta. 46 (1982): 1669-1673.

Pack et. al. “Chondrules With Peculiar REE Patterns: Implications for Solar Nebular Condensation at High C/O.” Science. Vol. 303. 13 Feb. 2004: 997-1000.

Thomas, R. “Part II: The Sample Introduction System.” A Beginner’s Guide to ICP-MS. 16(5) (2001): 56-60.

Thomas, R. “Part III: The Plasma Source.” A Beginner’s Guide to ICP-MS. 16(6) (2001): 26-3

Thomas, R. “Part VII: Mass Separation Devices – Double Focusing Magnetic-Sector Technology.” A Beginner’s Guide to ICP-MS. 16(11) (2001): 22-27.

Thomas, R. "Part XII: A Review of Interferences" A Beginner's Guide to ICP-MS. 17(10) (2001): 24-31.

Wanke et. al. "On the Chemistry of the Allende Inclusions and Their Origin as High Temperature Condensates." Earth and Planetary Science Letters. 23: (1974).

Wood, J.A. "Formation of Chondritic Refractory Inclusions: The Astrophysical Setting." Geochimica et Cosmochimica Acta. 68 (2004): 4007-4021.

Zanda, B. "Chondrules." Earth and Planetary Science Letters. 224: (2004): 1-17.

Appendix A:
Tables and Figures

Element Abundance Data Collected in the Various Studies that Kornacki and Fegley (1986) Cited in Their Research

Study	Nb	Ta	Nb/Ta	Zr	Hf	Zr/ Hf	Method of Analysis
Mason (1982)	3.9 ±5%	-	-	61 ±5%	1.9 ±5%	32 ±7%	Spark-Source Mass Spectromotry
Grossman (1977)	-	-	-	50 ±10%	-	-	Collected from a previous study
Wanke (1974)	6.6 ±20%	0.25 ±20%	26 ±28%	93 ±10%	3.3 ±10%	28 ±14%	Gamma-ray spectrometry
Grossman (1976)	-	0.29 ±42%	-	-	1.7 ±24%	-	Gamma-ray spectrometry

Table 1.1: Refractory element abundance data measured on CAIs from the various sources Kornaki and Fegley (1986) used to compile their values. Included are the abundance data (ppm), the study conducted, and the means of analysis. The values on this table represent the mean values as reported in these studies. The errors represent the largest error reported for any of the data obtained for that individual element.

Stoiciometry of the Primary Phases Found in the CAIs

Phase	Stiochiometry
Melilite	$Ca_2Al(Al,Si)O_7$ $Ca_2MgSi_2O_7$
Anorthite	$CaAl_2Si_2O_8$
Calcium-rich pyroxene (fassite)	$Ca(Mg,Al,Ti)(Al,Si)_2O_6$
Spinel	$MgAl_2O_4$

Table 2.1: The primary phases found within the CAIs analyzed via optical petrography and qualitative microprobe analysis and their relative stoichiometries.

Refractory Element Ratios for the Various Chondritic Constituents in Allende

Chondritic Constituent	Point Name	Nb/Ta ($1\sigma = 10\%$)	Zr/Hf ($1\sigma = 10\%$)
Matrix	Matrix1	16.2	34.7
	Matrix2	20.5	41.0
CAI in Sample 3529-63-RR1	B03	3.5	46.7
	B04	3.5	52.7
	B05	5.7	n.d.
	B06	2.7	63.8
	B07	3.3	49.7
	B08	7.1	56.8
	B09	4.9	39.1
	B10	4.0	41.1
	B11	3.4	46.2
	B12	4.6	n.d.
	B13	7.0	28.7
	B14	12.2	44.9
	B15	n.d.	n.d.
	B16	2.9	n.d.
CAI in Sample 3529-61-RR1	A05	2.0	n.d.
	A06	2.4	11.8
	A07	1.6	61.4
	A10	0.9	43.9
	A11	2.5	48.8
	A12	1.6	73.1
	A13	3.2	65.3
	A16	12.7	31.2
	A17	10.2	37.2
	A18	5.2	41.4
	A19	9.8	51.0
Chondrules	A7	22.3	38.1
		24.2	41.0
	A6	17.7	39.2
		16.3	39.2
	A5	10.4	30.4
	A4	3.8	39.4
	A3	10.0	37.6
		7.5	34.8
Bulk Solar System	Chondritic	19.9	34.3

Table 6.1: Refractory element ratios for single analysis points on the various chondritic constituents within the CV3 chondrite Allende obtained via LA-ICP-MS.

Elemental-Oxide Abundances in wt.% for the CAIs in Allende

Point	Na2O	CaO	MgO	Cr2O3	Al2O3	TiO2	P2O5	FeO	SiO2	Cl	MnO	SO3	K2O	Total
B03	0.361	17.487	3.879	0.075	33.751	0.942	0.064	0.095	43.529	0.009	0.065	0.013	0.009	100.274
B04	0.115	9.655	25.472	0.208	22.766	0.853	0.069	0.198	41.993	0.000	0.003	0.000	0.017	101.349
B05	5.414	14.751	1.730	0.185	25.437	0.414	0.102	2.026	32.673	0.205	0.094	0.010	0.454	83.448
B06	0.292	19.312	1.343	0.060	35.833	0.450	0.120	0.103	43.806	0.000	0.003	0.000	0.001	101.323
B07	0.061	7.371	26.126	0.589	32.654	0.650	0.071	0.195	32.307	0.000	0.022	0.008	0.000	100.054
B08	0.280	18.136	2.686	0.163	38.335	0.880	0.126	0.116	40.807	0.003	0.029	0.008	0.000	101.567
B09	0.044	6.792	17.790	1.059	47.863	1.758	0.081	0.179	23.320	0.000	0.069	0.000	0.000	98.955
B10	0.069	7.361	26.978	0.555	27.979	0.768	0.067	0.161	35.632	0.004	0.039	0.000	0.000	99.612
B11	0.046	8.352	24.636	0.533	28.586	0.841	0.043	0.183	36.370	0.000	0.067	0.000	0.000	99.656
B12	0.524	16.298	5.671	0.265	21.084	0.296	0.113	3.580	35.051	0.054	0.032	0.033	0.037	83.025
B13	0.019	0.856	26.390	1.511	62.731	1.678	0.033	0.561	9.633	0.000	0.056	0.011	0.005	103.485
B14	0.334	6.378	25.300	0.431	14.177	0.593	0.038	0.426	53.297	0.001	0.078	0.024	0.038	101.114
B15	0.703	16.086	5.670	0.139	34.571	0.236	0.084	0.387	42.702	0.003	0.037	0.024	0.061	100.703
B16	3.187	14.288	4.153	0.049	21.585	0.217	0.081	3.210	33.595	0.675	0.088	0.029	0.093	81.095
A05	0.055	26.062	12.276	0.033	15.587	2.515	0.122	0.101	43.082	0.028	0.020	0.035	0.010	99.920
A06	0.226	1.706	0.552	0.036	67.633	0.069	0.533	1.226	2.584	0.590	0.008	0.497	0.111	75.636
A07	0.032	0.552	26.553	0.148	69.400	0.431	0.062	0.088	0.712	0.024	0.021	0.019	0.004	98.041
A10	0.025	1.428	25.000	0.192	69.738	0.227	0.036	0.756	2.355	0.000	0.018	0.000	0.000	99.774
A11	0.216	35.791	1.978	0.000	26.383	0.218	0.190	0.264	34.598	0.109	0.026	0.034	0.000	99.782
A12	0.076	25.905	11.319	0.097	24.076	1.261	0.153	0.073	38.451	0.043	0.000	0.009	0.009	101.461
A13	0.011	2.145	25.878	0.140	70.226	1.922	0.036	0.155	0.979	0.006	0.000	0.000	0.008	101.504
A16	5.467	5.673	12.556	0.075	48.628	0.283	0.050	1.605	24.199	0.566	0.000	0.032	0.000	99.007
A17	0.123	23.472	0.458	0.014	4.922	0.016	0.177	25.883	45.572	0.037	0.106	0.084	0.000	100.855
A18	0.010	1.064	23.927	0.250	66.354	0.271	0.065	1.627	2.557	0.027	0.049	0.054	0.008	96.257
A19	0.000	25.590	17.630	0.050	2.794	0.331	0.131	0.357	53.513	0.009	0.014	0.008	0.000	100.424

Table 7.1: Elemental-oxide abundances in wt.% for the CAIs in Allende. The abundances were obtained via qualitative microprobe analysis with a beam diameter of 30 microns. The point names represent the various areas on Figures 3.1 and 3.2 where the beam was aimed at. They can additionally be compared with the LA-ICP-MS data obtained from the same points.

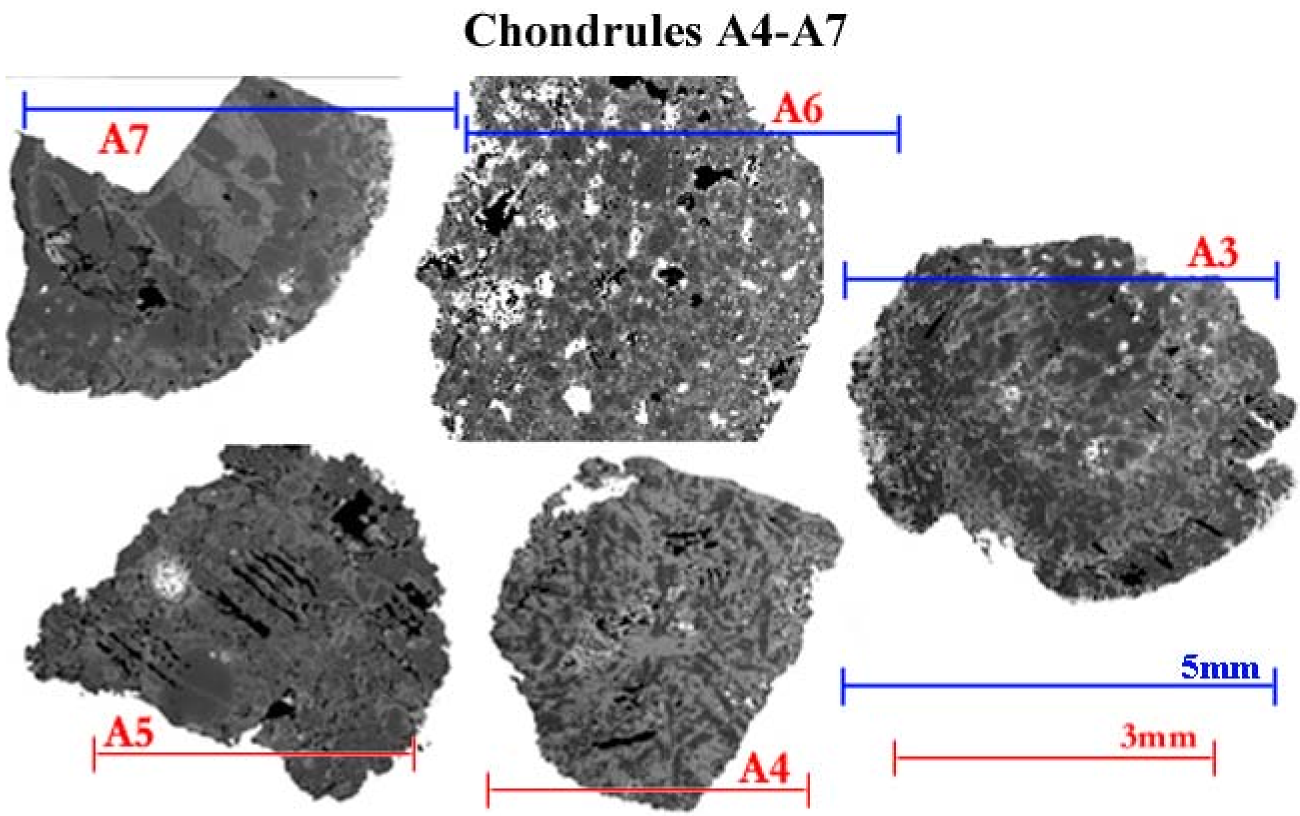

Figure 1.1: Backscattered electron (BSE) images of the five chondrules analyzed via electron microprobe.

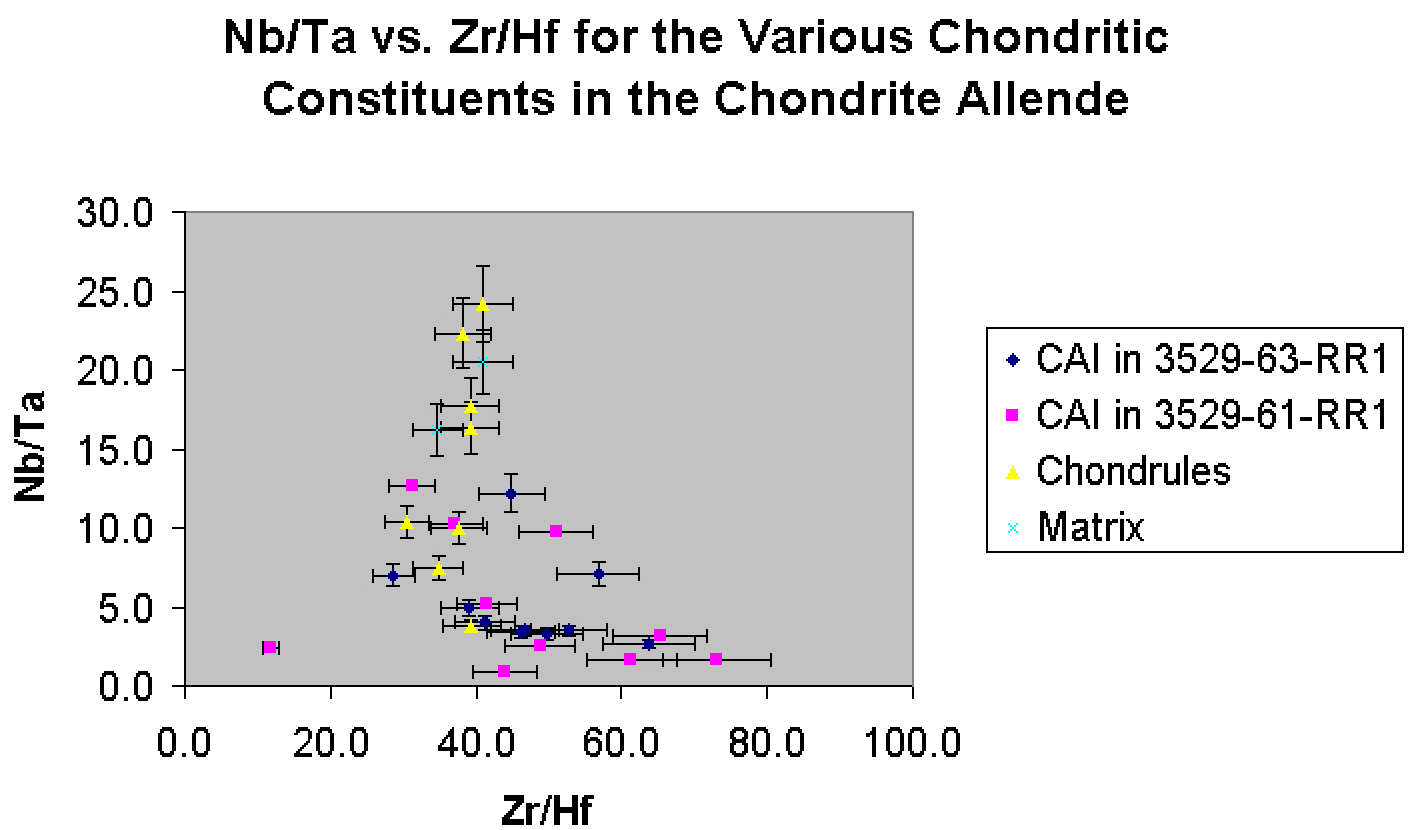

Figure 2.1: Nb/Ta values versus Zr/Hf ratios obtained via LA-ICP-MS for the various chondritic constituents studied.

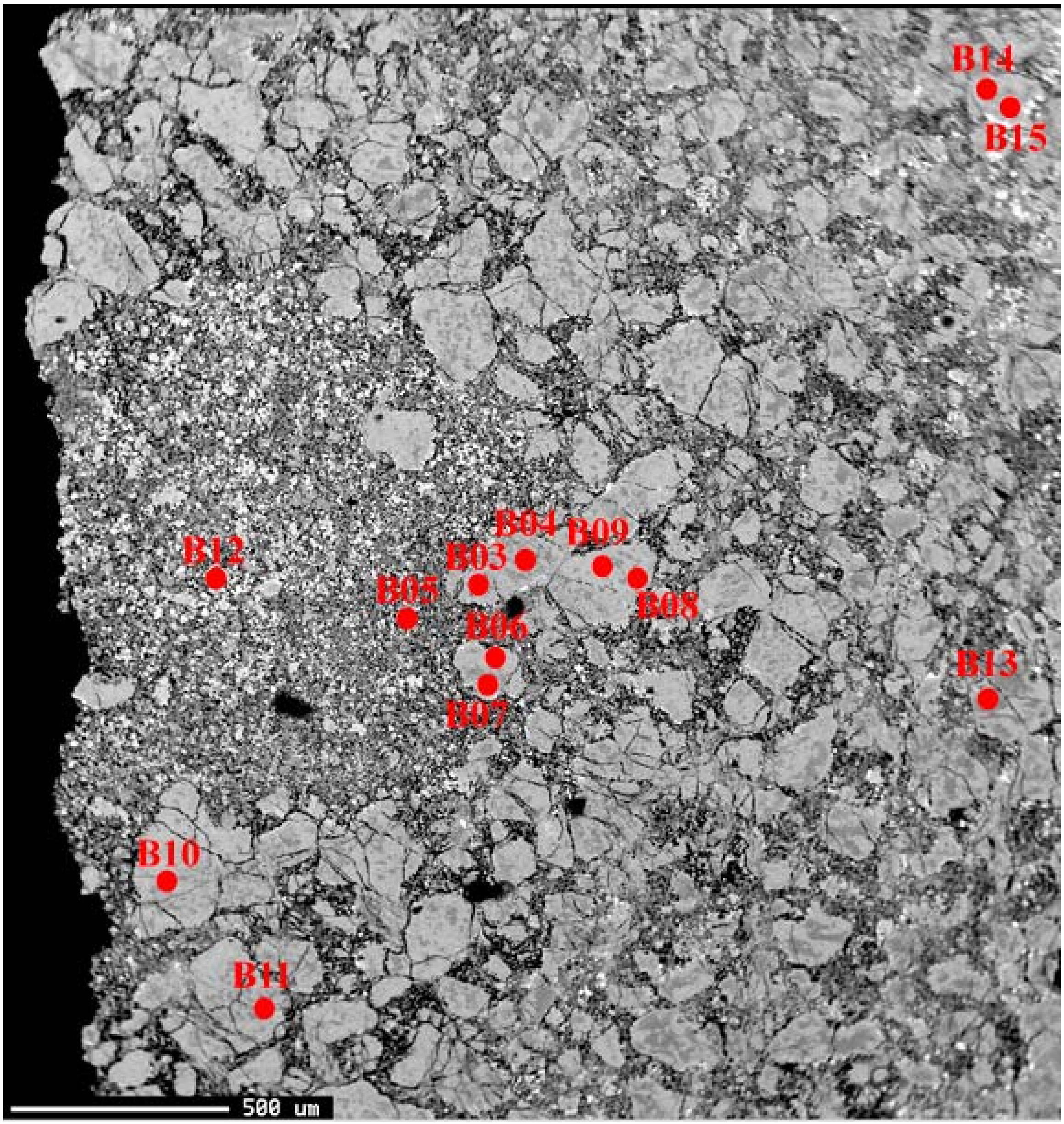

Figure 3.1: Backscattered Electron Image of the CAI in sample 3529-63-RR1. The red circles represent the points examined via LA-ICP-MS and qualitative microprobe analysis.

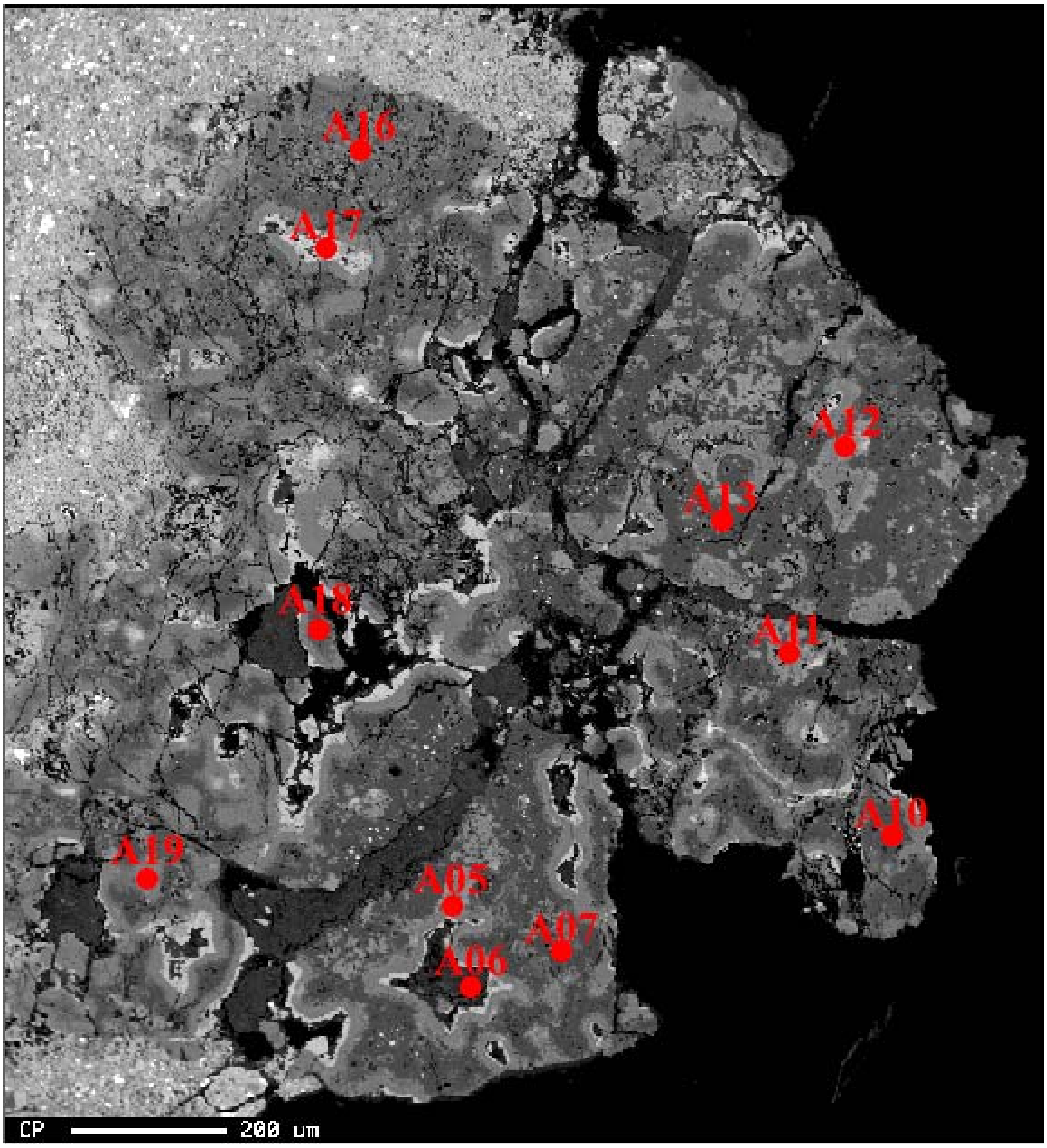

Figure 3.2: Backscattered Electron image of the CAI in sample 6529-61-RR1. The red circles represent the points examined via LA-ICP-MS and qualitative microprobe analysis.